Divalent cations can control a switch-like behavior in heterotypic and homotypic RNA coacervates

Paulo L. Onuchic[§a], Anthony N. Milin[§a], Ibraheem S. M. Alshareedah[b], Ashok A. Deniz*[a], Priya R. Banerjee*[b]

[a]Department of Integrative Structural and Computational Biology, The Scripps Research Institute, La Jolla, California 92037, USA

[b]Department of Physics, University at Buffalo, State University of New York, Buffalo, NY 14260, USA

§ These authors contributed equally

*Corresponding Authors: P. R. B.: prbanerj@buffalo.edu. A. A. D.: deniz@scripps.edu

Abstract

Liquid-liquid phase separation (LLPS) of RNA and protein plays a major role in the cellular function of membraneless organelles (MLOs). MLOs are sensitive to changes in cellular conditions, such as fluctuations in cytoplasmic ion concentrations. To investigate the effect of these changes on MLOs, we studied the influence of divalent cations on the physical and chemical properties of RNA coacervates. Using a model arginine-rich peptide-RNA system, we predicted and observed that variations in signaling cations exert interaction-dependent effects on RNA LLPS. Changing the ionic environment has opposing effects on the propensity for heterotypic and homotypic RNA LLPS, which results in a switch between coacervate types. Furthermore, divalent ion variations continuously tune the microenvironments and fluid properties of heterotypic and homotypic droplets. Our results may provide a generic mechanism for modulating the biochemical environment of RNA coacervates in a cellular context.

Introduction

Phase separation aids in regulating essential functions of cells and organisms. Within the cellular context, condensation-driven phase separation of biomolecules selectively compartmentalizes essential proteins, nucleic acids, and biochemical processes[1]. Liquid-liquid phase transitions can drive dynamic intracellular compartmentalization to form membrane-less organelles (MLOs) such as the nucleolus and stress granules[2–5]. Unlike their membrane-bound counterparts such as the nucleus, the unique physicochemical features of MLOs can enable liquid-like behavior such as facile formation, fusion, and dissolution[2]. These dynamic qualities provide a means for cells to sense and respond rapidly to changing environments, such as the cytoplasm during stress[2]. In this context, stimulus-dependent liquid-liquid phase separation (LLPS) of biopolymers has recently emerged with numerous implications in biology[6,7].

One of the driving forces of MLO formation is the weak multivalent interactions among proteins and nucleic acids[8]. Quantitative understanding and predictive control of the underlying interaction network are therefore key topics of research. The interchain associations of proteins and nucleic acids are largely determined by their primary sequences[8]. Intrinsically-disordered proteins (IDPs) with low-complexity repetitive sequences have been identified as drivers of MLO biogenesis, with charged sequences being one of the most common motifs found in intracellular MLOs[9]. Electrostatic interactions play a defining role in controlling the phase separation behavior of charged low-complexity sequences[8,10,11]. Phase separation *via* charge-charge interactions, commonly known as complex coacervation, can be recapitulated in an *in vitro* model consisting of an arginine-rich peptide and RNA[12,13]. Our recent work demonstrated that a peptide-RNA mixture can display reentrant phase behavior, where droplets can form and dissolve due to monotonic variation of ionic peptide-RNA ratios alone[13]. This type of behavior can be modeled simply using early polymer chemistry theories[14,15], with electrostatic interactions being the only effective interaction parameter. In addition to complex coacervation of RNA and IDPs, recent reports have observed liquid-liquid phase transitions *via* homotypic interactions of RNA chains in the absence of protein[16,17].

The global phase behavior of IDP-RNA mixtures is determined by a complex interplay between homotypic (IDP-IDP and RNA-RNA) and heterotypic (IDP-RNA) interactions. Hence, IDP-RNA mixtures can be sensitive to small changes in solution conditions such as temperature, ionic environment, pH, and IDP-RNA stoichiometry[8]. These alterations in physicochemical conditions can prompt dynamic responses in phase behavior by influencing the relative strengths and interplay of homotypic and heterotypic interactions. We reason that this interplay raises the possibility of an alternative stimulus-dependent LLPS modulation, *via* tuning of the relative magnitudes of competing interactions by solvent components.

Among the most regulated conditions in the cell is the cytoplasmic concentration of divalent ions[18–23]. Under rapidly changing cellular conditions, such as during stress, the flux of signaling cations coincides with MLO formation and dissolution dynamics[20–23]. We set out to determine how fluctuations in divalent ion concentrations could control the phase behavior of proteins and RNA. A recent study shows that the phase separation of a stress granule-related IDP, TIA-1, can be regulated by Zn^{2+} [24]. Our hypothesis is founded on the potential of divalent cations, such as Mg^{2+} and Ca^{2+}, to have a destabilizing effect on heterotypic IDP-RNA interactions while stabilizing homotypic RNA interactions. We anticipate that these opposing effects could give rise to a switch-like behavior with the capacity to regulate between complex coacervates (heterotypic) and RNA coacervates (homotypic) by simply modulating cation concentration in solution.

Additionally, the same underlying opposing effects on molecular interactions could also result in continuous tuning of droplet physical properties and composition.

A divalent cation has opposing effects on heterotypic (peptide-RNA) and homotypic (RNA-RNA) droplets

We previously studied important biophysical aspects (reentrant phenomena and non-equilibrium sub-compartmentalization) of LLPS using an *in vitro* model IDP-RNA system, consisting of an arginine-rich peptide {RP_3 (RRxxxRRxxxRRxxx)} and a long homopolymeric single-stranded RNA {polyU (800-1000 kDa)}[13]. This peptide-RNA system was chosen because it has been shown to be a valuable model for understanding the electrostatically-mediated phase behavior of intracellular ribonucleoprotein (RNP) granules[12], which often contain IDPs featuring arginine-rich motifs[9]. Our previous studies showed that monovalent (Na^+) cations reduce the propensity for phase separation in this system, which is consistent with the importance of heterotypic electrostatic interactions for LLPS in such RNP systems[13].

Here, we investigated the effects of divalent cations on the phase behavior of this system. Turbidity measurements at 350nm (Fig 1a), along with laser scanning confocal fluorescence microscopy at different salt concentrations (Fig 1b) confirmed that increased concentration of divalent (Mg^{2+}) cations reduced LLPS. This is expected due to a weakening of heterotypic electrostatic interactions between RP3 and RNA that drive complex coacervation of these oppositely charged biopolymers. This effect is similar to that of monovalent (Na^+) cations (Fig S3), though divalent ions are more effective.

We then tested the influence of divalent cations on homotypic phase separation of RNA. It is well known that the structure and assembly of both RNA and DNA are heavily influenced by the presence of divalent cations[25,26]. This has been especially well-studied for Mg^{2+}, which assists in the stabilization of RNA 3D structure, and has long been used in RNA folding and structural studies[25–27]. Therefore, in the case of polyU RNA, we anticipated that increased Mg^{2+} concentration could shield the electrostatic repulsion between the phosphate backbone of RNA and facilitate non-canonical U-U base pairing interactions[28–30], thus stabilizing droplet formation. Indeed, it has been shown that spermine and spermidine, which are small organic cations with 4+ and 3+ charges, respectively, can lead to polyU coacervation[31]. A recent report also showed that varying amounts of monovalent cations (Na^+) and a molecular crowder (PEG) can lead to phase separation of polyU[17]. In our system, we tested if variation of divalent cation concentration was sufficient to induce polyU coacervation in the absence of PEG. Using turbidity measurements, we investigated LLPS of polyU upon increasing Mg^{2+} and Ca^{2+} (Fig 1c). Solution turbidity data in conjunction with confocal fluorescence microscopy (Fig 1d) showed that polyU forms droplets in the presence of Mg^{2+} and Ca^{2+} in a concentration dependent manner, with Ca^{2+} showing a lower concentration threshold required for phase separation. These droplets displayed liquid-like characteristics such as fusion, circular appearance, and recovery of fluorescence after photobleaching (Fig 1, 4, S4, S5). Addition of PEG lowers the phase separation threshold concentration for polyU and Mg^{2+} (Fig S4), consistent with the known effect of PEG in nucleic acid cluster formation[32–34]. We observed polyU phase separation only at > 300 mM NaCl in the presence of PEG (Fig S4), suggesting that the multivalency of the cation is not necessary but does dramatically alter the phase separation threshold of polyU.

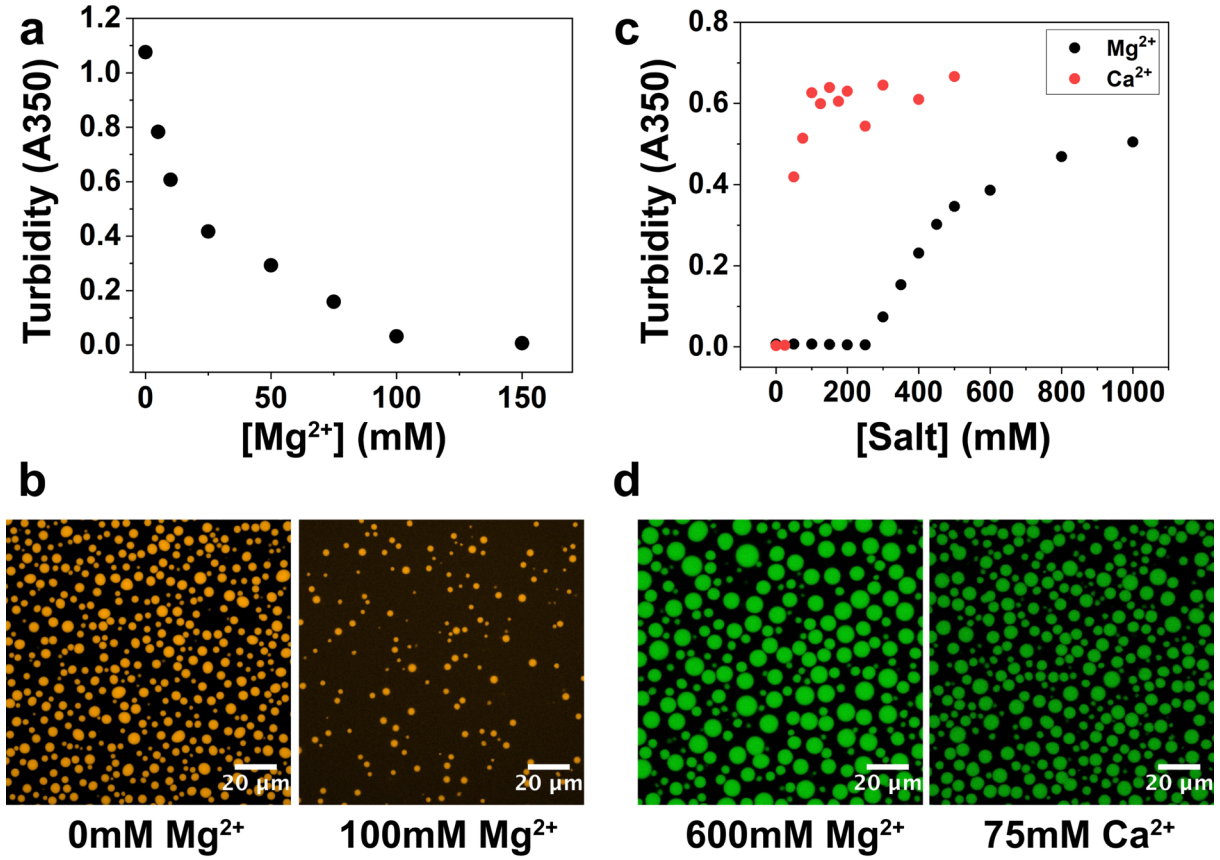

Figure 1: Increase in divalent cation concentration leads to dissolution of heterotypic RP3-polyU droplets and formation of homotypic polyU droplets. a. Solution turbidity measurements of RP3-polyU droplets as a function of [$MgCl_2$] ([RP3] = 500µM, 0.6x polyU wt/wt). **b.** Confocal fluorescence microscopy images of RP3-polyU droplets under different divalent salt conditions ([RP3] = 500µM, 0.6x polyU wt/wt, 0.5µM RP3-AF594). **c**. Solution turbidity measurements of polyU coacervates as a function of [$MgCl_2$] and [$CaCl_2$] (1mg/mL polyU). **d.** Confocal fluorescence microscopy image of polyU coacervates (1.5mg/mL polyU, 600mM $MgCl_2$, 0.5µM FAM-UGAAGGAC) (1.5mg/mL polyU, 75mM $CaCl_2$, 0.5µM FAM-UGAAGGAC).

Divalent salt triggers a switch-like phase behavior of a peptide-RNA system

The above results clearly demonstrate the opposing effects of divalent cations on homotypic and heterotypic phase separation in a peptide-RNA system. If the phase boundaries (Fig 1a, 1c) remain consistent in the combined RP3-polyU system, Mg^{2+} can act as a stimulus to create a switch-like phase behavior. In other words, starting with RP3-polyU droplets, a titration of Mg^{2+} would first lead to dissolution of these heterotypic droplets and subsequent formation of homotypic RNA droplets. Sequential turbidity measurements of RP3-polyU mixtures over increasing [Mg^{2+}] corroborated this prediction, displaying a window of miscibility between the two-phase regions of the phase diagram (Fig 2a). To more directly visualize switching between different regions of the phase diagram, we used confocal fluorescence microscopy with differentially labeled RP3 and RNA (Fig 2b). Starting with heterotypic RP3-polyU coacervates at low salt (10mM Tris, 0mM Mg^{2+}), we added 150mM Mg^{2+} into the solution, which resulted in the dissolution of the droplets. Subsequent addition of Mg^{2+} to a final concentration of 500mM produced new homotypic polyU droplets (Fig 2b). Given the orthogonal effects of Mg^{2+} on our system, we can conclude that these are two distinct types of polyU RNA droplets, which will

henceforth be referred to as heterotypic RP3-polyU droplets and homotypic polyU droplets. This behavior could also be recapitulated qualitatively using a Flory-Huggins based lattice model. This theory of polymer phase separation operates under the assumption that the net response of our peptide-RNA system is manifested by a superposition of heterotypic and homotypic interaction potentials (SI Note-1). Taken together, these data and analyses demonstrate an orthogonal phase behavior of this *in vitro* RNP system in response to a variation in Mg^{2+} concentrations.

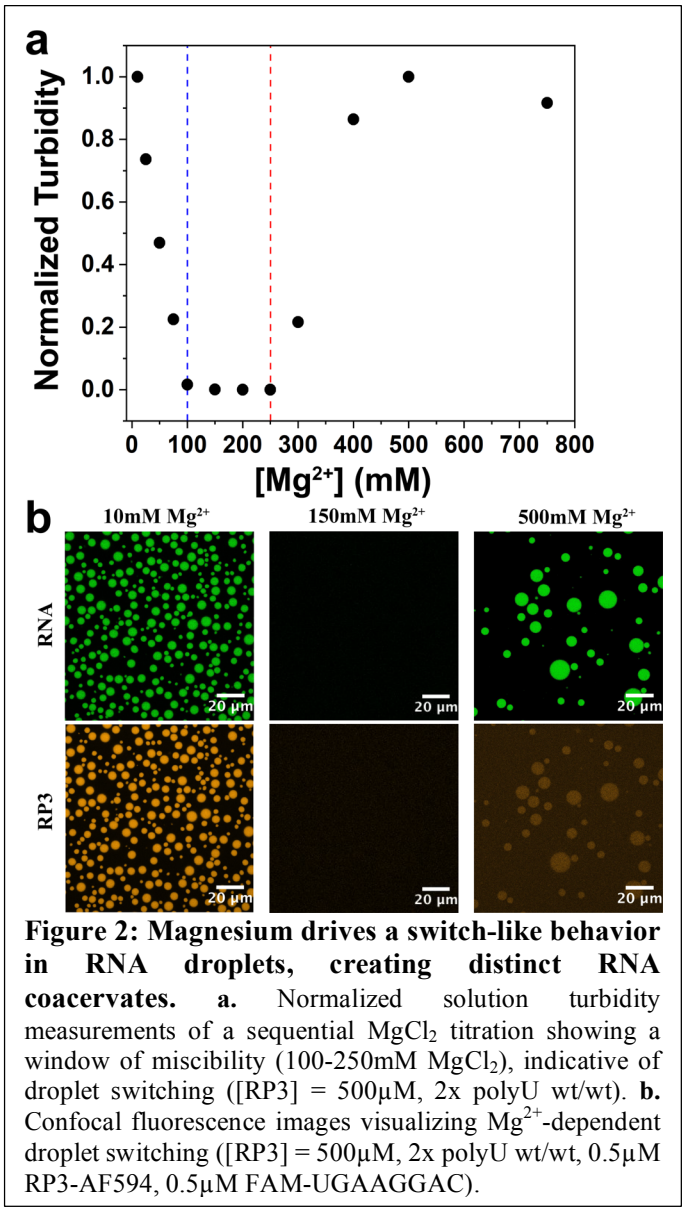

Figure 2: Magnesium drives a switch-like behavior in RNA droplets, creating distinct RNA coacervates. **a.** Normalized solution turbidity measurements of a sequential $MgCl_2$ titration showing a window of miscibility (100-250mM $MgCl_2$), indicative of droplet switching ([RP3] = 500µM, 2x polyU wt/wt). **b.** Confocal fluorescence images visualizing Mg^{2+}-dependent droplet switching ([RP3] = 500µM, 2x polyU wt/wt, 0.5µM RP3-AF594, 0.5µM FAM-UGAAGGAC).

Heterotypic peptide-RNA and homotypic RNA droplets offer functionally distinct microenvironments

During salt-induced switching from heterotypic RP3-polyU droplets to homotypic polyU droplets, we noticed that the partitioning of RP3 into droplets was dramatically reduced (Fig 2b). Since RNP droplets may function in concentrating cellular proteins and enzymes in an organelle-like microenvironment[35], any alterations in the selective partitioning of proteins and nucleic acids may be directly linked to their function. Based on a series of confocal imaging experiments, we calculated the estimated partitioning of a range of probes with variable molecular weight and charge using fluorescent RNA and peptides/proteins as partitioning markers (Tables S1-S3). We define partitioning as the ratio of fluorescence intensity between the dense and dilute phase (I_{dense}/I_{dilute}) (Fig S6). These probes were selected to feature molecular weights ranging from small organic molecules (< 1 kDa) to large globular proteins (~ 100 kDa), along with diversity in charge and structure.

Figure 2b demonstrates a high preferential inclusion of RP3 within heterotypic RP3-polyU droplets as expected. Upon increasing cationic concentration, we anticipate an exclusion of RP3 from homotypic polyU droplets due to charge screening of RP3-RNA interactions and a simultaneous strengthening of homotypic polyU interactions, as represented in Figure 3a. Experimentally, we observed a continuous decrease in RP3 partitioning into homotypic polyU droplets, eventually leading to preferential exclusion at 1500mM Mg^{2+} (Fig 3a). Although RP3 showed weak partitioning at 500mM Mg^{2+}, a peptide $(GR)_{20}$ (20 arginines) with significantly higher positive charge than RP3 (6 arginines) showed favorable partitioning even under these

conditions. However, $(GR)_{20}$ and RP3 partitioning both decreased with increasing Mg^{2+}, as expected due to charge screening (Fig 3a, Fig S6, Table S2). Along with the partitioning decrease, we saw partial selective exclusion of both RP3 and $(GR)_{20}$ at 1500mM Mg^{2+}. Additionally, we observed that an archetypal IDP, α-synuclein, positively partitioned within heterotypic RP3-polyU droplets, but is excluded from homotypic polyU droplets (Fig 3b, Table S3). A large globular fusion protein, eGFP-MBP, was excluded from both types of droplets, while a molecular chaperone from the small heat shock protein family, Hsp27, showed comparable partitioning properties to that of α-synuclein (Fig 3b, Table S3). Clear distinctions in partitioning properties between small RNA probes were also observed. U_{10} RNA partitioned well into the RP3-polyU droplets, but poorly into the homotypic polyU droplets (Table S3). A_{10} RNA, however, showed very strong partitioning into polyU droplets. These observed differences can be attributed to the sequence complementarity of A_{10} RNA, which can strongly interact with polyU, as compared to U_{10} RNA. The variation in partitioning among our probes in the homotypic and heterotypic droplets provides additional evidence that these droplets carry biochemically distinct microenvironments.

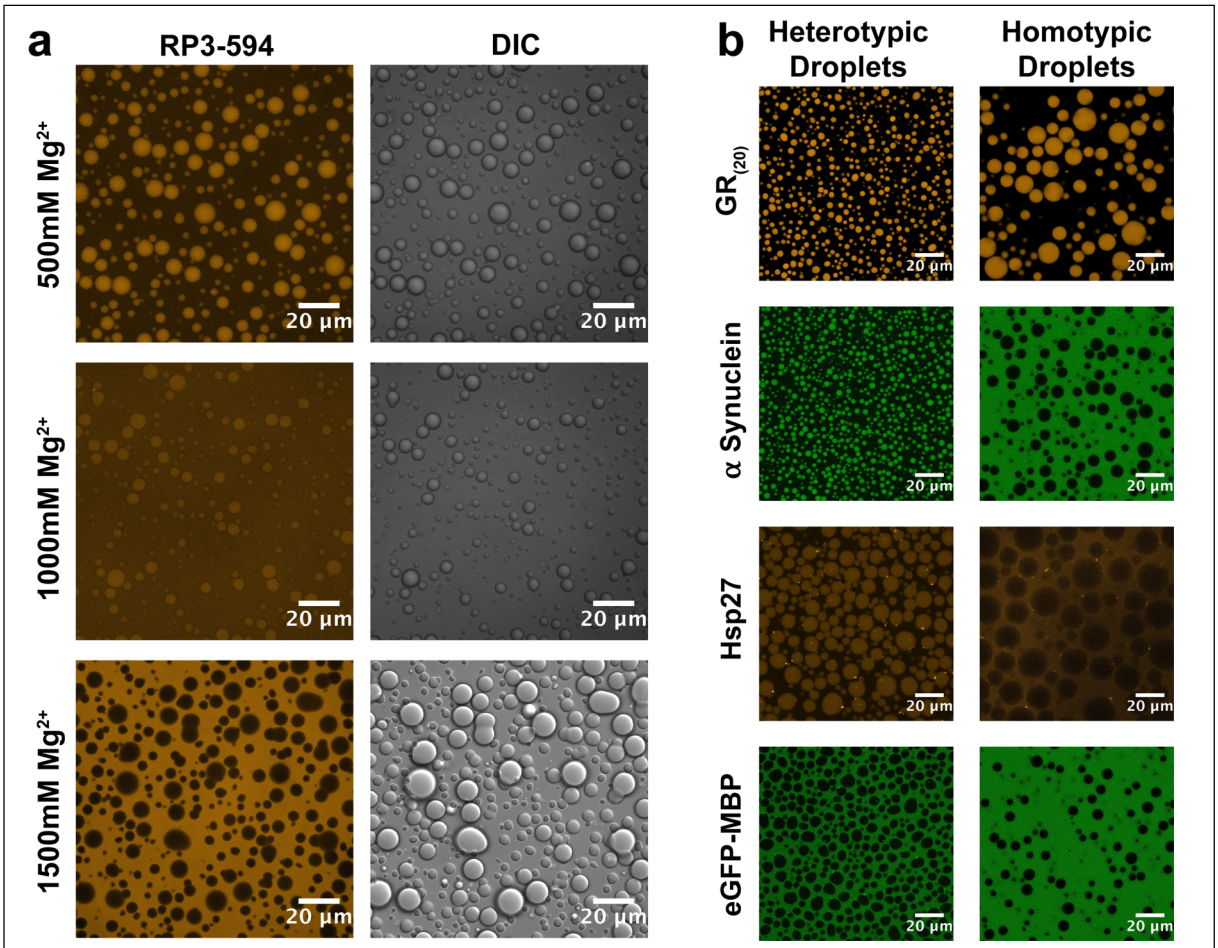

Figure 3: Heterotypic and homotypic droplets display distinct microenvironments. a. Confocal fluorescence and DIC images of polyU droplets with RP3-594 as a fluorescent probe (1.5mg/mL polyU, 0.5µM RP3-AF594). **b.** Confocal fluorescence images showing peptide/protein partitioning in heterotypic and homotypic RNA coacervates (Left Panels: [RP3] = 500µM, 0.6x polyU wt/wt, 10mM $MgCl_2$ - Right Panels: 1mg/mL polyU, 500mM $MgCl_2$) (Fluorescent probes: 0.5µM GR20-AF594, 0.5µM α-synuclein-AF488, 0.5µM Hsp27-AF594, 0.5µM eGFP-MBP-AF488).

Mg^{2+} controls the material properties of heterotypic and homotypic RNA droplets

The results above show that under certain conditions, a switch-like behavior between heterotypic and homotypic RNA droplets and their differing biochemical environments can be controlled by a simple variation in divalent ion concentration. We studied whether the same salt-dependent tuning of the heterotypic and homotypic interactions that are the molecular basis for this switching would also vary the material properties within each type of droplet. Based on the arguments presented earlier, we would again anticipate opposing effects for the two kinds of droplets upon increasing [Mg^{2+}], with a rise in fluidity of heterotypic RP3-polyU droplets and a drop in fluidity in homotypic polyU droplets. To test this idea, we used fluorescence recovery after photobleaching (FRAP) experiments, where the fluorescence recovery time (τ_{FRAP}) of an RNA probe (FAM-UGAAGGAC) was taken as a relative measure of molecular diffusivity and hence droplet fluidity under identical experimental conditions.

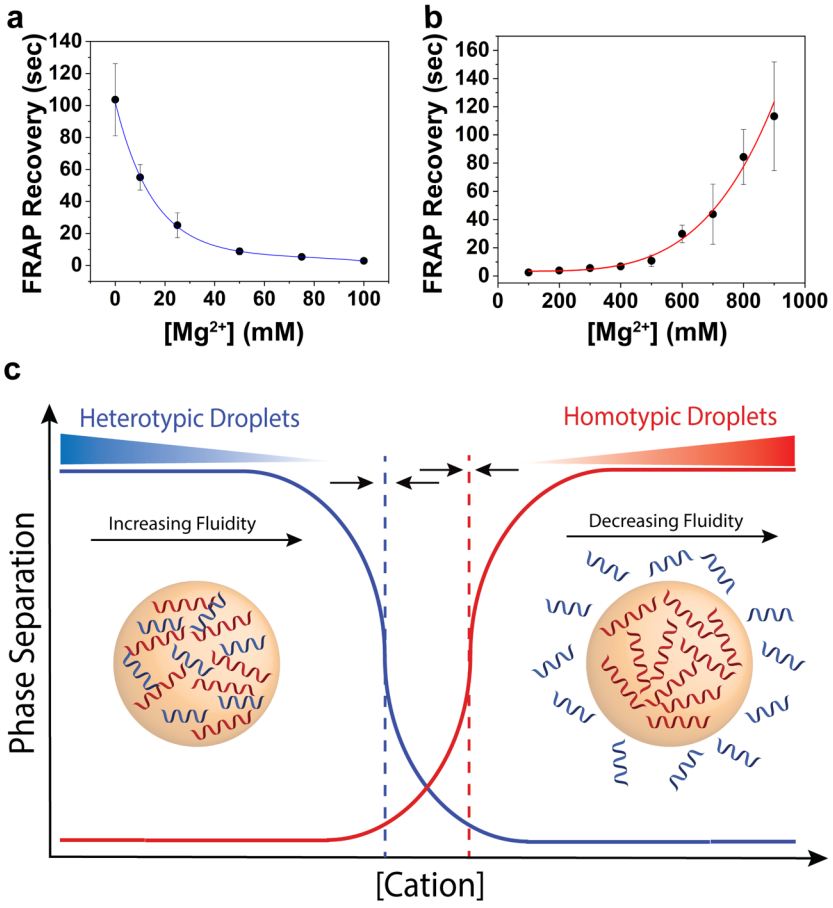

Figure 4: Magnesium concentration alters the fluidity of heterotypic and homotypic droplets. a. Fluorescence recovery in RP3-polyU droplets as a function of [$MgCl_2$]. ([RP3]=500μM, 0.6x polyU wt/wt). **b.** Fluorescence recovery in polyU droplets as a function of [$MgCl_2$] (2 mg/mL polyU, 10% PEG) **c.** Cartoon representation of switch-like behavior between heterotypic and homotypic droplets as a function of increasing cation concentration. The dotted lines represent the phase boundaries of the distinct droplet types. The arrows indicate that these phase boundaries will move under changing conditions and are capable of overlapping. In the cartoon, RNA is represented in red, while peptide/protein is represented in blue.

For RP3-polyU droplets, our results revealed that τ_{FRAP} decreases substantially from ~120 sec at 0mM Mg^{2+} to ~3 sec at 100mM Mg^{2+} (Fig 4a). We quantified the relative scaling of the τ_{FRAP} *vs.* [Mg^{2+}] for RP3-polyU coacervates, which revealed a scaling factor of -0.035 ± 0.0034 using a linear fit of the log-transformed recovery data (SI Note 2). This scaling component provides us with the means to characterize the sensitivity of fluidity to changes in magnesium concentration. Additionally, we showed a significant drop in preferential partitioning of this RNA probe between 10mM and 100mM Mg^{2+} (Table S1). The drop in fluidity is consistent in monovalent salt, with an increase in NaCl also resulting in decreased τ_{FRAP} (Fig S3). Together, these data show that salt-induced tuning of the electrostatic interactions substantially alters the physical properties of RP3-polyU coacervates.

We further probed for the relative fluidity of homotypic polyU droplets as a function of divalent salt concentration. Our hypothesized trend was observed, in that polyU coacervates undergo progressive hardening with increasing divalent salt concentration (Fig 4b). For example, above a concentration of 900mM Mg^{2+} and in the presence of 10% PEG, the FRAP recovery becomes difficult to quantify as the droplets transition towards a gel-like state with extremely low fluidity (Fig S9). Similar to the RP3-polyU coacervates, we defined the scaling here to quantitatively describe this variation with a scaling factor of 0.005 ± 0.00028, which is smaller than that of the RP3-polyU coacervates by a factor of ~7. This trend is consistent under similar conditions in the absence of PEG (Fig S5). Using the fluorescence intensity of the same RNA probe (FAM-UGAAGGAC), we observed increased RNA partitioning within the droplets as a function of increased [Mg^{2+}] (Table S1). These results suggest that at higher concentrations of Mg^{2+} the fraction of RNA increases within the dense phase. Since increasing [Mg^{2+}] drives progressive homotypic polyU droplet hardening, we hypothesized that sequestration of Mg^{2+} by a chelating agent would reverse this effect. To test this reversibility, we introduced EDTA in the system, which strongly chelates Mg^{2+} and decreases the bulk concentration of free [Mg^{2+}]. Our data revealed that the inclusion of EDTA decreased the FRAP time (Fig S5). Using microscopy, we show that the addition of EDTA to preformed droplets and subsequent addition of Mg^{2+} can reversibly dissolve and reassemble homotypic polyU droplets (Fig S5).

Discussion

Homotypic and heterotypic interactions are central in governing the LLPS of RNA-binding proteins containing low-complexity sequences. The feasibility of RNA phase separation by homotypic interactions increases the complexity by which these individual interactions are coupled in regulating the condensed phase dynamics of multi-component RNP granules[36]. In our work, we illuminated some of the aspects of this emerging complexity through the lens of physical and chemical property variations in a simplified model RNP granule. Using experimental results, supported by an analytical model, we showed that a model RNP granule is capable of undergoing a switch-like behavior in response to orthogonal RNA interactions. We were able to trigger this behavior in response to a single stimulus, which was the incorporation of divalent ions. Along with droplet switching, we showed selective and restrictive partitioning of biomolecules, as well as tunable material properties in our distinct condensed phases. Both the switching and tunable behaviors observed in this work can be predicted based on the opposing effects of divalent cations on heterotypic and homotypic interactions (Fig 4c, SI note-1). We anticipate that different conditions could alter the degree of overlap between the two phase-separation regimes, which would instead give rise to continuous tuning behavior. We explored this possibility for the case of Ca^{2+} ions, another important cellular divalent ion. In this case, the lower concentration stabilization of homotypic phase separation results in overlapping regimes and continuous variation in droplet composition (Fig S7). Furthermore, we observed the formation of dynamic substructure formation during the jump in Ca^{2+} concentration (Fig S8), reminiscent of vacuoles observed in our previous work[13].

The single stimulus-driven creation of distinct and tunable condensed phases, with unique chemical and physical properties, reveals potential biological implications. Interaction-based specificity of droplet components can dictate the composition of droplets *in vitro*, suggesting a potential explanation for the extensive variation in composition seen among cellular RNA granules[36–39]. Such a stimulus-dependent modulation of liquid-liquid phase separation may also provide valuable insights into how intracellular RNP granules are regulated in response to versatile

environmental cues. As alluded to previously, one motivation for studying divalent cations and their effect on phase separation in our system was the effect of fluctuations in cytoplasmic ion concentrations. Work in the field of ion signaling and homeostasis has shown that changes in ion concentration in cellular compartments are involved in major cellular pathways, such as stress signaling and transcription[18–24]. Variations in cellular Mg^{2+} and Ca^{2+} also have significant relevance in a variety of functions, including timekeeping, neuronal migration and signaling[19–21,23]. Of special interest to us was the evidence pointing to the rising cytoplasmic concentration of divalent ions during stress, as recent work in phase separation showed that monovalent salt concentration plays a role in stress granule formation[10,40]. Our work reveals what could be an essential role for divalent ion concentration in this process, tuning not only the material properties of these droplets, but also the accessibility of important biological molecules to specific condensed phases. Specifically, these emergent properties could be necessary in segregation and protection of essential RNAs during cellular stress[41,42]. We note that the divalent ion-mediated tuning and switching discussed here is likely one key mechanism contributing to the tunability of cellular MLOs. Other types of specific and non-specific interactions between cellular RNA and proteins will therefore be able to alter these effects, providing for a rich tunability and inclusion specificity that can studied in the future. Additionally, understanding the interactions and microenvironments that regulate the phase separation of simple RNAs and peptides could help reveal the necessary components and interactions in the formation of protocells, as coacervate biochemistry is a promising direction in deciphering the origin of cells. Lipid membrane vesicles have been proposed as suitable compartments in self-replicating ribozyme systems in a prebiotic RNA world[43]. Homotypic RNA phase separation may provide important advantages as an alternative compartmentalization mechanism. These advantages include stable formation under high divalent ion concentrations needed for ribozyme function[43], facile exchange of nucleotides, and selective RNA compartmentalization based on specific interactions. Combined, these results reveal a way to consider regulation of LLPS in cellular environments as a complex integration and tuning of weak interactions, which are dependent but also influential to the cellular microenvironment.

Acknowledgements

We gratefully acknowledge support for this work from NIGMS/NIH (Grants RO1 GM066833 and RO1 GM115634 to A.A.D.) and National Science Foundation (Grant MCB 1818385 to A.A.D.) and from University at Buffalo, SUNY, College of Arts and Sciences to P.R.B. We thank Ian J. Macrae, Irem Nasir, Emily Bentley, and Jose Luis Olmos Jr. for valuable feedback regarding this work. We thank Emily Bentley for providing the eGFP-MBP used in the study.

Author contributions

P.L.O., A.N.M., P.R.B, and A.A.D. designed the study. P.L.O., A.N.M., and P.R.B. designed the experimental strategies. P.L.O. and A.N.M. collected and analyzed all turbidity, confocal microscopy, partitioning, and FRAP data. P.R.B. generated the recombinant proteins and performed protein fluorescence labeling. P.L.O. and A.N.M. performed peptide fluorescence labeling. I.A. constructed the analytical model and performed the free energy surface simulation. All authors contributed in writing the manuscript.

References

1. Banani, S. F., Lee, H. O., Hyman, A. A. & Rosen, M. K. Biomolecular condensates: Organizers of cellular biochemistry. *Nature Reviews Molecular Cell Biology* **18,** 285–298 (2017).
2. Hyman, A. A., Weber, C. A. & Jülicher, F. Liquid-Liquid Phase Separation in Biology. *Annu. Rev. Cell Dev. Biol.* **30,** 39–58 (2014).
3. Holehouse, A. S. & Pappu, R. V. Functional Implications of Intracellular Phase Transitions. *Biochemistry* **57,** 2415–2423 (2018).
4. Boeynaems, S. *et al.* Protein Phase Separation: A New Phase in Cell Biology. *Trends Cell Biol.* **28,** (2018).
5. Shin, Y. & Brangwynne, C. P. Liquid phase condensation in cell physiology and disease. *Science* **357,** (2017).
6. Ruff, K. M., Roberts, S., Chilkoti, A. & Pappu, R. V. Advances in Understanding Stimulus-Responsive Phase Behavior of Intrinsically Disordered Protein Polymers. *Journal of Molecular Biology* (2018). doi:10.1016/j.jmb.2018.06.031
7. Aguzzi, A. & Altmeyer, M. Phase Separation: Linking Cellular Compartmentalization to Disease. *Trends in Cell Biology* **26,** 547–558 (2016).
8. Mittag, T. & Parker, R. Multiple Modes of Protein–Protein Interactions Promote RNP Granule Assembly. *Journal of Molecular Biology* (2018). doi:10.1016/j.jmb.2018.08.005
9. Boeynaems, S. *et al.* Phase Separation of C9orf72 Dipeptide Repeats Perturbs Stress Granule Dynamics. *Mol. Cell* **65,** 1044–1055.e5 (2017).
10. Molliex, A. *et al.* Phase Separation by Low Complexity Domains Promotes Stress Granule Assembly and Drives Pathological Fibrillization. *Cell* **163,** 123–133 (2015).
11. Mitrea, D. M. *et al.* Self-interaction of NPM1 modulates multiple mechanisms of liquid-liquid phase separation. *Nat. Commun.* **9,** (2018).
12. Aumiller, W. M. & Keating, C. D. Phosphorylation-mediated RNA/peptide complex coacervation as a model for intracellular liquid organelles. *Nat. Chem.* **8,** 129–137 (2016).
13. Banerjee, P. R., Milin, A. N., Moosa, M. M., Onuchic, P. L. & Deniz, A. A. Reentrant Phase Transition Drives Dynamic Substructure Formation in Ribonucleoprotein Droplets. *Angew. Chemie - Int. Ed.* **56,** 11354–11359 (2017).
14. Flory, P. J. *Principles of Polymer Chemistry*. (Cornell University Press, 1953).
15. Overbeek, J. T. G. & Voorn, M. J. Phase separation in polyelectrolyte solutions. Theory of complex coacervation. *J. Cell. Comp. Physiol.* (1957). doi:10.1002/jcp.1030490404
16. Jain, A. & Vale, R. D. RNA phase transitions in repeat expansion disorders. *Nature* **546,** 243–247 (2017).
17. Van Treeck, B. *et al.* RNA self-assembly contributes to stress granule formation and defining the stress granule transcriptome. *Proc. Natl. Acad. Sci.* **115,** 2734–2739 (2018).
18. Berridge, M. J., Bootman, M. D. & Roderick, H. L. Calcium signalling: Dynamics, homeostasis and remodelling. *Nature Reviews Molecular Cell Biology* **4,** 517–529 (2003).
19. Romani, A. M. P. Intracellular magnesium homeostasis. *Magnes. Cent. Nerv. Syst.* **512,** 13–58 (2011).
20. Ross, W. N. Understanding calcium waves and sparks in central neurons. *Nature Reviews Neuroscience* **13,** 157–168 (2012).

21. Chaigne-Delalande, B. & Lenardo, M. J. Divalent cation signaling in immune cells. *Trends in Immunology* **35,** 332–344 (2014).
22. Clapham, D. E. Calcium Signaling. *Cell* **131,** 1047–1058 (2007).
23. Feeney, K. A. *et al.* Daily magnesium fluxes regulate cellular timekeeping and energy balance. *Nature* **532,** 375–379 (2016).
24. Rayman, J. B., Karl, K. A. & Kandel, E. R. TIA-1 Self-Multimerization, Phase Separation, and Recruitment into Stress Granules Are Dynamically Regulated by Zn2+. *Cell Rep.* **22,** 59–71 (2018).
25. Onoa, B. & Tinoco, I. RNA folding and unfolding. *Current Opinion in Structural Biology* **14,** 374–379 (2004).
26. Draper, D. E., Grilley, D. & Soto, A. M. Ions and RNA Folding. *Annu. Rev. Biophys. Biomol. Struct.* **34,** 221–243 (2005).
27. Lipfert, J., Herschlag, D. & Doniach, S. Riboswitch conformations revealed by small-angle X-ray scattering. *Methods Mol. Biol.* **540,** 141–159 (2009).
28. Wang, Y. X., Huang, S. & Draper, D. E. Structure of a U-U pair within a conserved ribosomal RNA hairpin. *Nucleic Acids Res.* **24,** 2666–2672 (1996).
29. Baeyens, K. J., De Bondt, H. L. & Holbrook, S. R. Structure of an RNA double helix including uracil-uracil base pairs in an internal loop. *Nat. Struct. Biol.* **2,** 56–62 (1995).
30. SantaLucia, J., Turner, D. H. & Kierzek, R. Stabilities of Consecutive A•C, C•C, G•G, U•C, and U•U Mismatches in RNA Internal Loops: Evidence for Stable Hydrogen-Bonded U•U and C•C+ Pairs. *Biochemistry* **30,** 8242–8251 (1991).
31. Aumiller, W. M., Pir Cakmak, F., Davis, B. W. & Keating, C. D. RNA-Based Coacervates as a Model for Membraneless Organelles: Formation, Properties, and Interfacial Liposome Assembly. *Langmuir* **32,** 10042–10053 (2016).
32. Desai, R., Kilburn, D., Lee, H. T. & Woodson, S. A. Increased ribozyme activity in crowded solutions. *J. Biol. Chem.* **289,** 2972–2977 (2014).
33. Kilburn, D. *et al.* Entropic stabilization of folded RNA in crowded solutions measured by SAXS. *Nucleic Acids Res.* **44,** 9452–9461 (2016).
34. Tyrrell, J., Weeks, K. M. & Pielak, G. J. Challenge of Mimicking the Influences of the Cellular Environment on RNA Structure by PEG-Induced Macromolecular Crowding. *Biochemistry* **54,** 6447–6453 (2015).
35. Li, X. H., Chavali, P. L., Pancsa, R., Chavali, S. & Babu, M. M. Function and Regulation of Phase-Separated Biological Condensates. *Biochemistry* **57,** 2452–2461 (2018).
36. Van Treeck, B. & Parker, R. Emerging Roles for Intermolecular RNA-RNA Interactions in RNP Assemblies. *Cell* **174,** 791–802 (2018).
37. Aulas, A. *et al.* Stress-specific differences in assembly and composition of stress granules and related foci. *J. Cell Sci.* **130,** 927–937 (2017).
38. Benarroch, E. E. Cytoplasmic RNA granules, ribostasis, and neurodegeneration. *Neurology* **90,** 553–562 (2018).
39. Ditlev, J. A., Case, L. B. & Rosen, M. K. Who's In and Who's Out—Compositional Control of Biomolecular Condensates. *Journal of Molecular Biology* (2018). doi:10.1016/j.jmb.2018.08.003
40. Bounedjah, O. *et al.* Macromolecular crowding regulates assembly of mRNA stress granules after osmotic stress: New role for compatible osmolytes. *J. Biol. Chem.* **287,**

2446–2458 (2012).

41. Namkoong, S., Ho, A., Woo, Y. M., Kwak, H. & Lee, J. H. Systematic Characterization of Stress-Induced RNA Granulation. *Mol. Cell* **70,** 175–187.e8 (2018).
42. Langdon, E. M. & Gladfelter, A. S. A New Lens for RNA Localization: Liquid-Liquid Phase Separation. *Annu. Rev. Microbiol.* **72,** 231–254 (2018).
43. Müller, U. F. Re-creating an RNA world. *Cellular and Molecular Life Sciences* **63,** 1278–1293 (2006).